Electronic Supplementary Material (ESI) for ChemComm.

Supplementary Information

Spectroscopic Observation and Structure-Insensitivity of Hydroxyls on Gold

Yiteng Zheng,[1] Yue Qi,[2] Ziyu Tang,[2] Junzhi Tan,[1] Bruce E. Koel,*[1] Simon G. Podkolzin*[2]

[1]Department of Chemical and Biological Engineering, Princeton University, Princeton, New Jersey 08544, United States

[2]Department of Chemical Engineering and Materials Science, Stevens Institute of Technology, Hoboken, New Jersey 07030, United States

*Corresponding Authors: BEK: bkoel@princeton.edu, SGP: Simon.Podkolzin@Stevens.edu

1. Catalyst Preparation

Catalysts were prepared using the incipient wetness impregnation (IWI) method by depositing gold (III) chloride ($HAuCl_4$, Sigma-Aldrich, 99.99% trace metal basis) on two supports: ZSM-5 zeolite (Si/Al=15, Zeolyst International CBV 3024E) and SiO_2 (CABOT, Cab-O-Sil HS-5 fumed silica). The Au loading was varied between 0.25 and 3.5 wt %. Prior to impregnation, the zeolite support was converted from the initial ammonium form to the hydrogen form (H-ZSM-5) via calcining in air by ramping the temperature at 5 K/min to 875 K and holding at this temperature for 4 h. After impregnation, the catalysts were dried under static air at room temperature overnight and then by ramping the temperature at 1 K/min to 393 K and holding for 4 h. After drying, the catalysts were calcined in flowing synthetic dry air (Airgas, Zero Grade) by ramping the temperature at 5 K/min to 673 K and holding for 2 h.

2. Reaction Testing

Reaction rate measurements for ethanol oxidation with oxygen in the gas phase were performed in a flow reactor system. About 0.1 g of an undiluted catalyst sample was loaded into a stainless steel tube with an outside diameter of ¼ inch that served as the reactor. The reactor was fitted with steel cloth filters (mesh size 40×40, McMaster-Carr) and quartz wool (fine nominal wool, Technical Glass Products) at the top and bottom of the catalyst bed to fix the position of the catalyst. A K-type thermocouple was placed to directly touch the reactor wall at the location of the catalyst bed. The reactor was placed inside a Mellen MTSC Microtherm vertical split furnace. The flow rates of gas-phase reactants, O_2 (Praxair, UHP 4.3, 99.993%) and He (Praxair, UHP 5.0, 99.999%), were controlled using Bronkhorst mass flow controllers. The flow rate of liquid-phase ethanol (Sigma Aldrich, ACS spectrophotometric grade) was

maintained at a constant value of 0.02 ml/min using a Scientific System Series III high-performance liquid chromatography (HPLC) pump.

Prior to testing, a catalyst sample was dried in situ in a 50-sccm He flow by increasing the temperature at 1 K/min from room temperature to 393 K and holding at this temperature for 2 h. After drying, the reactor temperature was allowed to decrease to 333 K. After the temperature stabilized at 333 K, a flow of liquid ethanol was started. Ethanol was vaporized at 373 K in a preheater filled with high-surface area quartz wool. The vaporized ethanol was mixed in a T-joint with a 50-sccm He flow, and the flow rate was allowed to stabilize for 15 min. Then the gas feed was switched to 32 mol % O_2/He with a total flow rate of 92 sccm. The moment of O_2 introduction was taken as the start of the time on stream. Reaction products were analyzed every 30 min with online sampling using a Varian-450 gas chromatograph (GC) equipped with both a thermal conductivity detector (TCD) and a flame ionization detector (FID). To avoid condensation of liquid products, the sampling line from the reactor to the GC was maintained at 473 K using a heating tape (rope heater, Omega FGR 100). The heating tape was wrapped outside the stainless steel tube and insulated with a 1-inch layer of glass wool. The reaction conditions were chosen to limit the ethanol conversion to less than 5% so that a differential reactor model could be used. Reaction rates are reported based on three separate runs for each catalyst.

3. In situ Diffuse Reflectance Infrared Fourier Transform Spectroscopy (DRIFTS)

DRIFTS spectra were collected using a Bruker INVENIO FTIR spectrometer equipped with a liquid nitrogen cooled mercury-cadmium-telluride (MCT) detector, a Harrick Praying Mantis diffuse reflection accessory and a Harrick Praying Mantis high temperature reaction chamber equipped with two ZnSe windows. About 0.02 g of an undiluted sample was loaded in

the reaction chamber and dehydrated in a 20-sccm flow of synthetic dry air by raising the temperature at a rate of 10 K/min to 573 K and holding for 1 h. The temperature was then lowered to 373 K, and the spectra were collected at this temperature under the same dry air flow with a resolution of 4 cm^{-1} by averaging 200 scans. The IR peak intensities were normalized relative to the Si-O-Si overtone peak at 1380 cm^{-1}, which was treated as constant for all samples.

4. X-Ray Diffraction (XRD)

XRD patterns of the catalysts were collected using a Bruker D8 Discover Diffractometer with Cu Kα radiation at a wavelength λ of 0.15406 nm, operated at 40 kV and 40 mA, over a 2θ range of 10-50° with a step size of 2° min^{-1}. The size of Au nanoparticles (L) was estimated using the Scherrer equation: $= \frac{K\lambda}{\beta \cos\theta}$, where K is the shape factor (0.89 dimensionless), and β is the peak width. The XRD pattern of bulk Au, used for comparison in Figures 1 and S1, was generated using a bulk Au unit cell in Materials Studio 2017 software by Dassault Systèmes BIOVIA, and this pattern matches experimental results in crystallographic databases.

5. Transmission Electron Microscopy (TEM)

TEM measurements were performed with a FEI TALOS F200X instrument operated at 200 kV. A sample powder with supported Au particles was ultrasonicated in ethanol first. Then, a few droplets of the produced suspension were placed on a carbon-coated copper grid. Afterwards, the sample was allowed to dry at room temperature in a vacuum oven. Particle size distributions were obtained by analyzing at least 100 metal particles using ImageJ version 1.53 software by the National Institutes of Health.

The metal dispersion, D, was calculated using the following equation:

$$D = 6\frac{v_{Au}/a_{Au}}{d_{avg}},$$

where v_{Au} is the volume of a single Au atom (0.0169 nm^3), a_{Au} is the surface area of an Au atom (0.0875 nm^2), and d_{avg} is the average particle size obtained from the TEM measurements.

6. Density Functional Theory (DFT) Calculations

Geometries and vibrational frequencies of hydroxyls on multiple Au surfaces were obtained with the DMol^3 DFT code in Materials Studio 2017 software by Dassault Systèmes BIOVIA. The spin-polarized calculations used the double numerical with polarization (DNP) basis set and the generalized gradient-corrected revised Perdew–Burke–Ernzerhof (GGA RPBE) functional. Tightly bound core electrons for Au were represented with semicore pseudopotentials. A density mixing fraction of 0.2 for the charge with direct inversion in the iterative subspace (DIIS) and orbital occupancy with thermal smearing of 0.005 Ha were used. The orbital cutoff distance of 0.44 nm was set for all atoms.

Three types of Au models were used. The first type was isolated Au clusters: Au_3, Au_5, Au_7, Au_{13} and Au_{55} (Figure 2). In these calculations, positions of all atoms were optimized.

The second type was periodic Au surfaces: Au(511), Au(211), Au(111) with a Au adatom and Au(111). The unit cells of these surfaces shown in Figure 2 were generated from a bulk crystal using an optimized Au lattice constant of 0.4250 nm with a vacuum spacing of 4 nm in the *c* direction. All unit cells had 3×3 surface atoms with 5 layers for a total of 45 Au atoms, except for the Au(111) with an Au adatom that had the unit cell with 46 Au atoms. To keep an even number of electrons in each model, an H atom in a threefold Au site was added to the

Au(111) with an Au adatom surface. The adsorbed H atom and OH did not share bonding Au atoms. The top three layers were optimized with hydroxyls during geometry optimization, accounting for surface relaxation. The remaining two bottom layers were constrained, accounting for the effect of the bulk structure. Reciprocal space integration over the Brillouin zone for the periodic models was approximated through k-point sampling with a separation of 0.4 nm^{-1} using the Monkhorst-Pack grids: (1×3×1) for Au(511) as well as Au(211) and (3×3×1) for Au(111) with an Au adatom as well as for Au(111).

The third model type was a Au_5 cluster inside a zeolite pore (Figure 1b). The cluster was anchored on a double Al-atom framework site in a 10-T ring. This site was generated by replacing two Si atoms in the T-8 and T-12 positions with Al atoms. The 10-T ring was selected in the middle of a periodic supercell that contained two full MFI unit cells ($Si_{192}O_{384}$) with lattice constants a=2.0022, b=1.9899 and c=1.3383 nm. The 10-T ring and its boundary O atoms were treated as the DFT, quantum mechanics (QM), region. The rest of the MFI supercell was treated as the molecular mechanics (MM) region. The QM calculations used the same DFT settings as those employed in the cluster and periodic surface calculations. The MM region was calculated with the GULP program using the Broyden-Fletcher-Goldfarb-Shanno (BFGS) optimization method and a universal force field (UFF). In the QM/MM calculations, positions of all atoms were optimized.

Vibrational frequency calculations were performed with a full Hessian for all atoms for the isolated clusters and bulk surfaces. A partial Hessian for the OH/Au_5 atoms was used in the QM/MM calculations. The vibrational frequencies are reported as calculated using the harmonic oscillator approximation, without adjustment.

Table S1. Vibrational frequencies calculated for hydroxyls on Au surfaces in Figure 2, cm^{-1}

	Au_5/ ZSM-5	Au_3	Au_5	Au_7	Au_{13}	A_{55}	Au(511)	Au(211)	Au(111) with Au adatom	Au(111)
ν_a(Au-O)	505	525	257	340	233	240	248	266	493	195
ν_s(Au-O)			374	376	350	311	321	323		308
δ(Au-OH)	846	843	692	705	649	556	614	628	820	588
			758	807	735	752	750	746		623
ν(O-H)	3695	3705	3684	3683	3686	3684	3686	3687	3689	3668

Table S2. Bond distances calculated for hydroxyls on Au surfaces in Figure 2, nm

	Au_5/ ZSM-5	Au_3	Au_5	Au_7	Au_{13}	A_{55}	Au(511)	Au(211)	Au(111) with Au adatom	Au(111)
Au-O	0.204	0.202	0.222 0.222	0.218 0.218	0.223 0.229	0.226 0.227	0.226 0.226	0.224 0.224	0.205	0.232 0.232
O-H	0.098	0.098	0.098	0.098	0.098	0.098	0.098	0.098	0.098	0.098

Table S3. Catalysts characterization and reaction testing results for ethanol oxidation with gas-phase oxygen

	Au loading, wt %	Au dispersion, %	Au surface area, $\mu mol_{Au}/g_{catalyst}$	C_2H_5OH conversion, %	Product selectivity, %			
					CH_3CHO	CH_3COOH	$CH_3COOC_2H_5$	CO/CO_2
Au/ZSM-5	0.25	100	13	3	40	12	48	0
Au/SiO_2	3.6	7	13	1	32	23	43	0

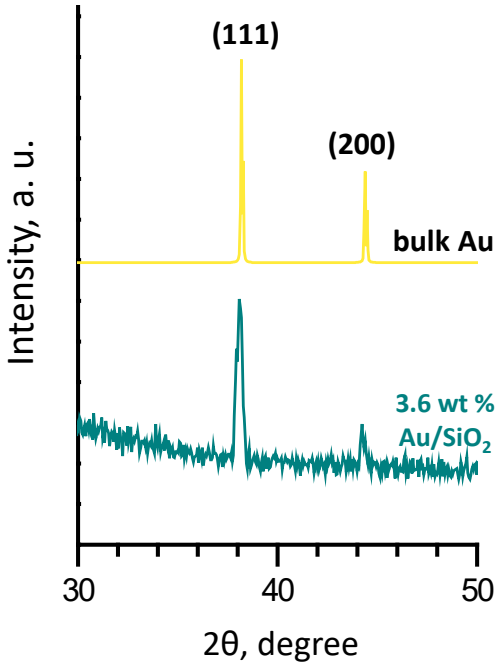

Figure S1. XRD patterns for 3.6 wt % Au/SiO_2 and bulk Au.

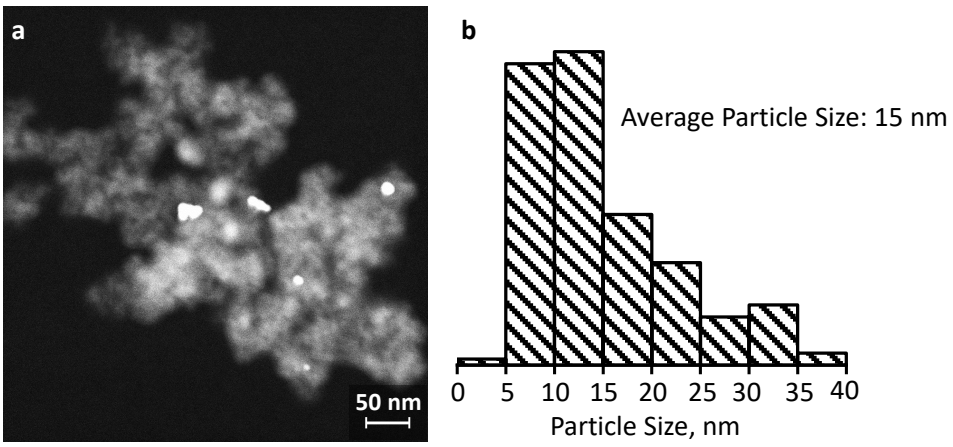

Figure S2. (**a**) TEM image for 3.6 wt % Au/SiO_2 in Figure 3c at a different scale with multiple Au particles visible, (**b**) Au particle size distribution histogram for 3.6 wt % Au/SiO_2 based on multiple TEM images with a total count of 185 Au particles.